Peer-reviewed version available at Sensors 2018, 18, 3972; doi:10.3390/s18113972

Article

NiFe alloy reduced on graphene oxide for electrochemical non-enzymatic glucose sensing

Zhe-Peng Deng[1,2], Yu Sun[3], Yong-Cheng Wang[1,*] and Jian-De Gao[4]

[1]College of Chemistry and Chemical Engineering, Northwest Normal University, Lanzhou 730070, P. R. China; dengzp516@163.com (Z.D.); ycwang@163.com (Y.W.)
[2]Gansu Computing Center, Lanzhou 730030, P. R. China; dengzp516@163.com
[3]Experiment Center of Northwest University for Nationalities, Lanzhou 730030, P. R. China; sunyu794@163.com
[4]Gansu University of Chinses Medicine, Lanzhou 730000, P. R. China; 13919124704@163.com
*Correspondence: ycwang@163.com; Tel.: +86-931-7971989

Abstract: NiFe alloy nanoparticles/graphene oxide hybrid (NiFe/GO) was prepared for electrochemical glucose sensing. The as-prepared NiFe/GO hybrid was characterized by transmission electron microscopy (TEM) and X-ray diffraction (XRD). The results indicated that NiFe alloy nanoparticles can be successfully deposited on GO. The electrochemical glucose sensing performance of the as-prepared NiFe/GO was studied by cyclic voltammetry and amperometric measurement. Results showed that NiFe/GO modified glassy carbon electrode had sensitivity of 173 μA $mM^{-1}cm^{-2}$ for glucose sensing with a linear range up to 5 mM, which was superior to commonly used Ni nanoparticles. Furthermore, high selectivity for glucose detection can be achieved by NiFe/GO. All the results demonstrated that NiFe/GO hybrid was promising for using in electrochemical glucose sensing.

Keywords: NiFe alloy; graphene oxide; glucose; non-enzymatic sensor

1. Introduction

Glucose sensing is important in many fields, such as medical diagnostics and food industry [1]. The earliest glucose sensing is reported by Clark and Lyons in 1962 using biological enzyme [2]. Since then, biological enzymes such as glucose oxidase and glucose dehydrogenase have been widely used for glucose sensing. However, the biological enzymes are susceptible to external condition such as temperature, humidity, pH, and so on, which lead to unstability of biological enzymes [3–5]. The expensive price and complicated mobilizing methods of biological enzymes also restrict its application [6]. Therefore, to address these problems, the research focus has been transfered to develop electrochemical non-enzymatic glucose sensors.

Due to its high stability and sensitivity, non-enzymatic electrochemical technology is a good choice for glucose sensing [7]. Various nanoparticles have been reported for constructing electrochemical non-enzymatic biosensors, such as noble metal Pt nanoparticles (Pt NPs) [3,8,9], Au NPs [10,11], Pd NPs [12,13], etc. However, the expensive price of these noble metals restricts their practical application. Furthermore, noble metals constructed electrochemical glucose sensors are usually poisoned by chloride ion containing widely in body's blood [14]. In order to exploit cheap electrochemical non-enzymatic glucose biosensors, considerable attention has been focusing on non-noble metal materials, such as Ni NPs [15–17], $Co(OH)_2$ nanotubes [18], Cu NPs [19,20], etc. Recent studies reveal that bimetallic materials [21], especially bimetal alloys, exhibit better catalytic performance than that of monometallic counterparts [22]. Xu et al. and Chen et al. both found that Pt-Ni alloy exhibited enhanced sensitivity for glucose sensing [23,24]. Besides, PtRu alloy [25], PtAu alloy [26], PtCo alloy [27], CoCu alloy [28], and NiCo alloy [29] have been used in glucose sensing.

Peer-reviewed version available at Sensors 2018, 18, 3972; doi:10.3390/s18113972

A support material is also important in electrochemical glucose sensor [30]. Carbon based materials (especially carbon nanotube and graphene) have extensively used to load the electrochemical catalyst due to its excellent conductivity, such as loading cupric oxide [31] or growing copper nanoparticles [32] on carbon nanotubes (CNTs) for electrochemical glucose sensing. Graphene and its oxide (graphene oxide, GO) have triggered researchers' interest since 2004 because of their good electrical conductivity and large specific surface area. Due to these exceptional properties, Graphene and GO have been chosed as supporting material in electrochemistry [33]. GO loaded with NiS [34], NiCo alloy [29] and CuS NPs [35] have been applied for electrochemical glucose sensing.

Based on the above considerations, we tried to study the alloying of commonly used Ni NPs in the scope of glucose detection with Fe element on GO, because NiFe alloy shows high electrochemical performance in various processes [36–39]. To the best of our knowledge, the NiFe alloy nanoparticles/graphene oxide hybrid (NiFe/GO) has never been reported for electrochemical glucose sensing. The NiFe/GO reveals better electrocatalytic performance towards glucose oxidation than the commonly used Ni NPs. High performance of NiFe alloy nanoparticles and superior conductivity of GO endow the NiFe/GO biosensor to electrochemically sensing glucose in wide concentration range.

2. Materials and Methods

2.1. Chemicals and reagents

All reagents used in experiments were analytical grade. Graphite powder was purchased from Alfa Aesar. Nickel sulfate hexahydrate, iron sulfate heptahydrate, hydrazine hydrate (80 wt%) and glucose are procured from Sinopharm Chemical Reagent Co., Ltd. Ascorbic acid (AA), uric acid (UA), and dopamine (DA) were purchased from ACROS. Deionized water (18.2 MΩ·cm) was used in all experiments.

2.2. Preparation of GO

GO was prepared by modified Hummers method [40]. 2 g Graphite and 1 g $NaNO_3$ were mixed with 50 mL H_2SO_4 (95%) in a 250 mL flask within an ice bath to keep a low temperature (Caution: ice bath is important and necessary). Then, 6 g $KMnO_4$ was added slowly into the above suspension with vigorous stirring. In this adding process, the reaction temperature should be kept lower than 20 °C. After that, the mixture was stirred at room temperature overnight. At the end, 60 mL H_2O was added slowly with vigorous agitation. The reaction temperature was increased rapidly up to 95 °C, and the color of suspension changed to yellow. Then, 10 mL of 30% H_2O_2 was added to the mixture. Finally, the obtained product was washed by rinsing with 5% HCl and then deionized water for several times until the pH of filtrate reached 7. After dry in vacuum dryer, gray powder GO was obtained.

2.3. Preparation of NiFe/GO composites

For the preparation of NiFe/GO composite (for example, the ratio of Ni to Fe is 1:1, denoted as NiFe/GO), 0.1 g of the as-prepared GO, 278.1 mg $FeSO_4{\cdot}7H_2O$ (1 mmol) and 262.9 mg $NiSO_4{\cdot}6H_2O$ (1 mmol) were added to 10 mL deionized water. The mixture was sonicated for 30 min to get an evenly dispersed solution. Then, 15 mL hydrazine hydrate was dropped slowly into the above solution followed by refluxing at 100 °C for 3 h under N_2 atmosphere. After reaction, the obtained NiFe/GO composite was washed using deionized water for several times. Finaly, the washed NiFe/GO composite was dried in vacuum for further use. Other composites (different Ni to Fe mass ratios, such as Ni_1Fe_4/GO, Ni_4Fe_1/GO, Ni/GO and Fe/GO) were prepared by adjusting the ratio of Ni and Fe. NiFe alloy NPs were also prepared for comparison using the same method without adding GO.

2.4. Preparation of the NiFe/GO hybrid modified electrode

5 mg NiFe/GO hybrid was dispersed in 1 mL solution that containing 0.5 mL ethyl alcohol and 0.5 mL deionized water. The above solution was sonicated for 30 minutes to get an evenly dispersed mixture. After sonicating, a certain amount of the mixture was dropped onto bare glassy carbon electrode (GCE) followed by adding 2 μL Nafion solution (0.5%) to entrap the NiFe/GO. The prepared electrode was denoted as NiFe/GO/GCE. For comparing, Ni/GO/GCE, Fe/GO/GCE and NiFe/GCE were fabricated similarly.

2.5. Apparatus and measurements

The morphologies of NiFe/GO composite were collected with a Tecnai G^2F^{30} electron microscope. XRD data were conducted on a Rigaku D/max-2400 diffractometer operating at a voltage of 40 kV and a current of 40 mA using Cu-K radiation as the X-ray source. Electrochemical characterization was performed on a CHI 660C electrochemical workstation with the modified GCE as working electrode, Pt wire as counter electrode and Ag/AgCl (3 M KCl) as reference electrode. All voltages used in the manuscript were versus to Ag/AgCl (3 M KCl) electrode.

3. Results and discussion

3.1. Structural characterization

The TEM image of the NiFe/GO is displayed in Figure 1. As shown in Figure 1a that NiFe alloies with diamter of about 100 nm are loaded on GO. Figure 1b-d show the element mapping of NiFe alloy. It can be seen clearly that Ni and Fe element are evenly distributed in NiFe alloy. This prove the successful preparation of NiFe alloy. Figure 3 shows the XRD pattern of NiFe/GO to further investigate the crystalline structure. The diffraction patterns located 44.5°, 51.9° and 76.4° can be ascribed to the diffraction of (111), (200), and (220) crystal planes of the NiFe alloy, respectively [41]. No peaks of GO can be found due to its small amount.

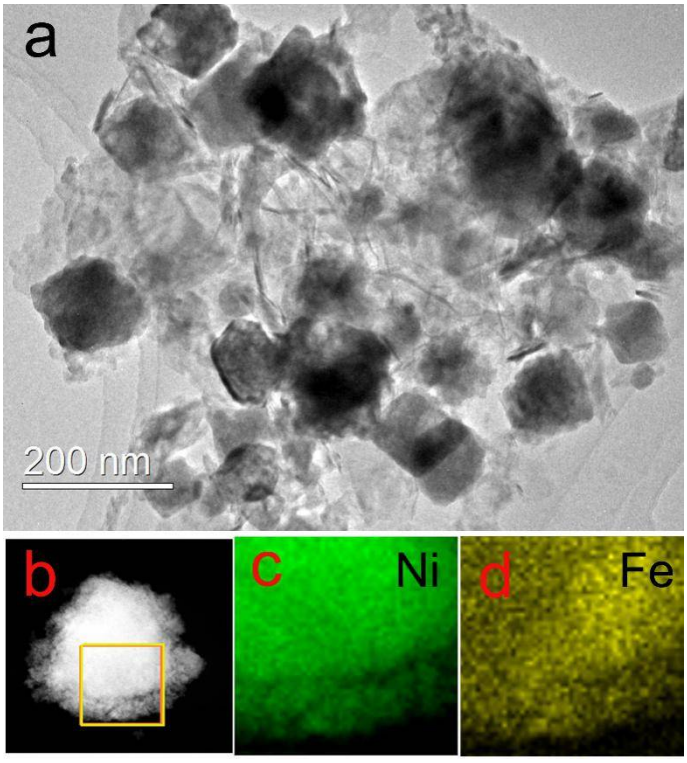

Figure 1. (a) TEM image of the NiFe/GO and (b, c d) element mapping of NiFe alloy.

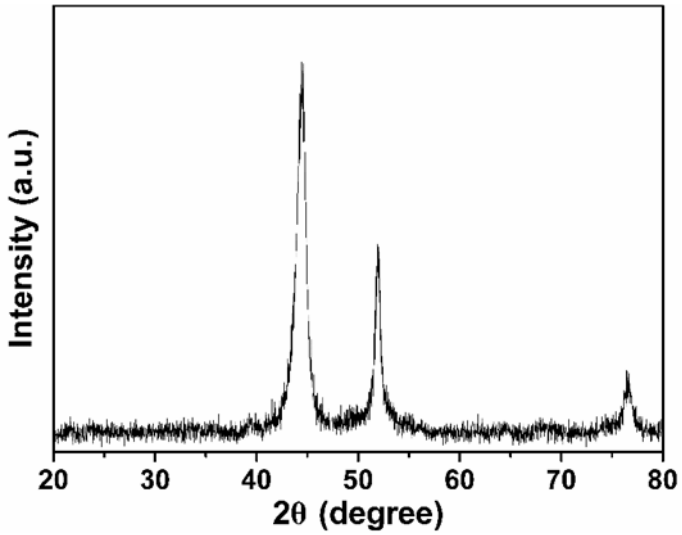

Figure 2. XRD pattern of NiFe/GO.

3.2. Electrochemical measurements

Figure 3 shows the typical cyclic voltammograms of the as-prepared GCE, Fe/GO/GCE, Ni/GO/GCE and NiFe/GO/GCE in 0.1 M NaOH solution in the presence of 1.0 mM glucose. It can be seen from Figure 3 that GCE and Fe/GO/GCE show very small current in the whole voltage range. Oxidation peaks between 0.50 to 0.55 V can be observed for Ni/GO/GCE and NiFe/GO/GCE, which can be ascribed to the oxidation of Ni^{2+} to Ni^{3+}. The Ni^{3+} accounts for the oxidation of glucose [15]. When Fe was added to Ni to form NiFe alloy, the current increases obviously. This indicates that NiFe alloy have higher performance for electrochemical glucose detection.

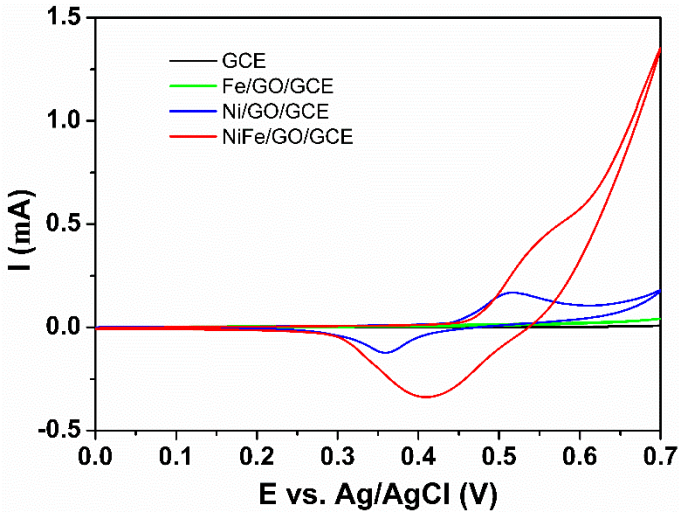

Figure 3. CVs of GCE, Fe/GO/GCE, Ni/GO/GCE and NiFe/GO/GCE in 0.1 M NaOH solution in the presence of 1.0 mM glucose at a scan rate of 10 mV/s.

To illustrate the effect of GO, the performance of NiFe/GCE and NiFe/GO/GCE were investigated. As shown in Figure 4, NiFe/GCE has only negligible current and the redox peaks can be seen in the inset figure. NiFe/GO/GCE shows much larger current than that of NiFe/GCE, indicating GO is important in the composite electrode. The GO not only acts as support to load NiFe alloy from aggregation, but also plays an important role for electronic transmission.

Peer-reviewed version available at Sensors 2018, 18, 3972; doi:10.3390/s18113972

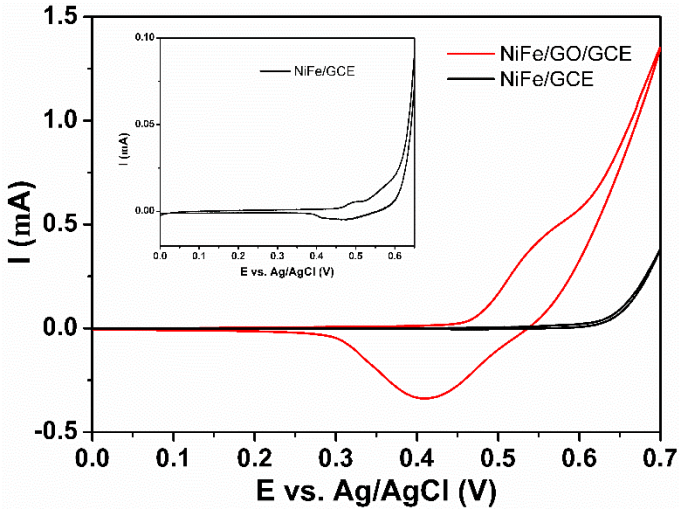

Figure 4. CVs of NiFe/GCE and NiFe/GO/GCE in 0.1 M NaOH solution in the presence of 1.0 mM glucose at a scan rate of 10 mV/s. Inset: CV of NiFe/GCE.

Furthermore, the effect of the ratio between Ni and Fe elements were investigated. As shown in Figure 5, Ni_1Fe_4/GO/GCE shows the smallest current. With the increase of Ni amount, NiFe/GO/GCE shows the biggest current. More Ni amount, instead, decrease the current as Ni_4Fe_1/GO/GCE shows. So, NiFe/GO/GCE was used for further research.

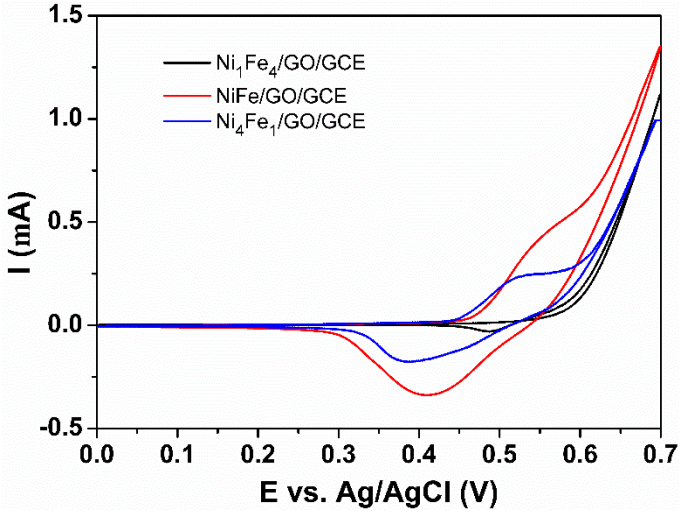

Figure 5. CVs of Ni_1Fe_4/GO/GCE, NiFe/GO/GCE and Ni_4Fe_1/GO/GCE in 0.1 M NaOH solution in the presence of 1.0 mM glucose at a scan rate of 10 mV/s.

In order to improve the electrocatalytic performance of NiFe/GO/GCE, the loading amount of NiFe/GO were studied. Figure 6 shows CV curves of NiFe/GO/GCE with different amount of NiFe/GO loading on GCE. It can be seen that the current increases gradually from the loading amount of 30 to 60 μg NiFe/GO. When the loading amount exceeding 60 μg, the current decreases. So, 60 μg is the optima loading amount and used in the later experiments. This phenomenon can be explained by the change of catalytic sites. At first, increasing loading amount of the NiFe alloy increased catalytic sites. However, overmuch loading amount limited mass transfer process, leading to the decrease of current [19].

Cyclic voltammetric measurements were performed at increased scan rates to better understand the electrocatalytic properties of the NiFe/GO/GCE for glucose oxidation. As demonstrated in Figure 7a, cathodic peak currents of NiFe/GO/GCE increased with the increasing scan rate. Figure 7b give the relationship between cathodic peak current and scan rate. It can be seen that cathodic peak currents increases linearly with the used scan rates. This result manifested

Peer-reviewed version available at Sensors 2018, 18, 3972; doi:10.3390/s18113972

159 the rate determining step was surface reaction control rather than diffusion control, which is
160 favorable for quantitative analysis.

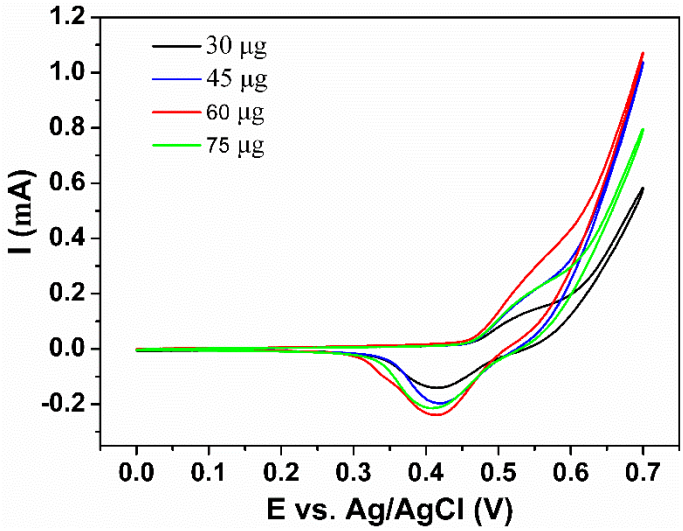

161

162 Figure 6. The effect of modificaion amount on the performance of electrode.

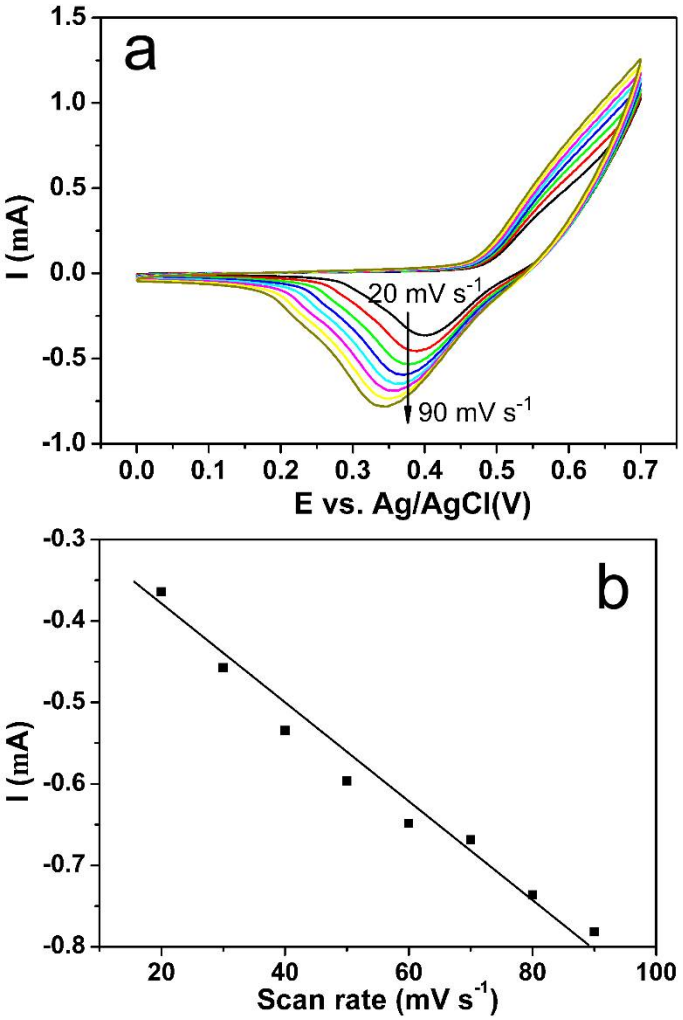

163

164 Figure 7. (a) Cyclic voltammograms of NiFe/GO/GCE at different scan rates from 20 to 90 mV/s in 0.1
165 M NaOH with 1.0 mM glucose. (b) Plot of cathode current vs the scan rate.

3.3. Amperometric response towards glucose sensing

Amperometric measurement was carried out to show the current response of the NiFe/GO/GCE towards continuously adding of various concentrations of glucose, which was carried out in vigorous stirred electrolyte. As shown in figure 8a, the NiFe/GO/GCE generates fast current response upon the addition of glucose from 50 to 400 μM everytime. According to the amperometric current, the corresponding calibration curve was plotted in Figure 8b. It can be seen that the NiFe/GO/GCE sensor showed a wide linear sensing range form 0 to 5 mM (R^2 = 0.9994), and a sensitivity of 173 μA $mM^{-1}cm^{-2}$. The high sensitivity can be ascribed to the high electrocatalytic activity of NiFe alloy and excellent electronic transmission performance of GO.

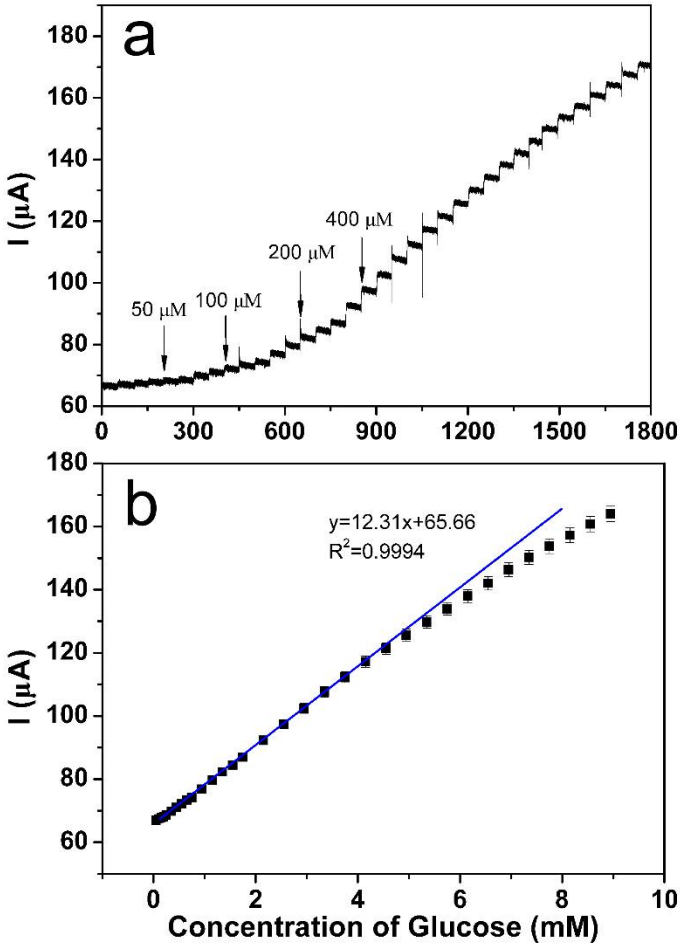

Figure 8. (a) Amperometric currents measured with continuous addition of glucose from 50 to 400 μM at 0.55 V for NiFe/GO/GCE. (b) The corresponding calibration curve.

3.4. Specificity and reproducibility of the NiFe/GO/GCE

DA, AA and UA are co-exist in human blood, which will influence the electrochemical non-enzymatic glucose sensing. To investigate the effect of DA, AA and UA on the glucose sensing, amperometric response test was carried out. Figure 9 shows the amperometric response current with addition of DA, AA, UA and glucose. It can be seen that the current generated by DA, AA and UA in mormal physiological concentration are only 4.1%, 1.9% and 2.6% compared to that of glucose, respectively. This research demonstrates that the NiFe/GO/GCE possesses specificity for glucose sensing and can be used in reality sensing.

Peer-reviewed version available at Sensors 2018, 18, 3972; doi:10.3390/s18113972

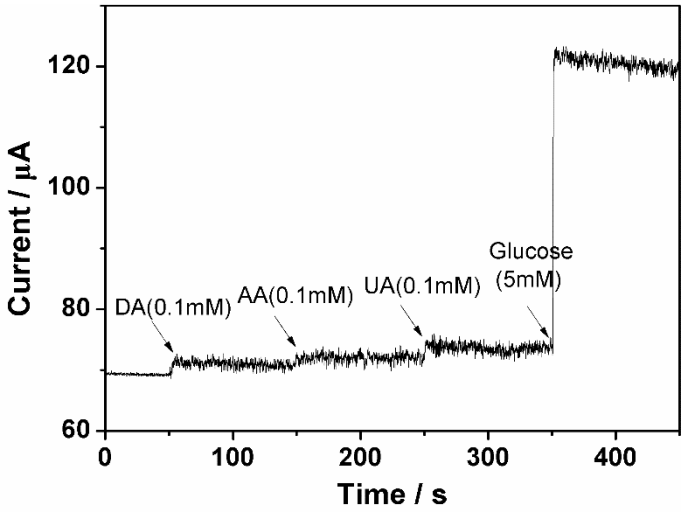

Figure 9. Amperometric response of NiFe/GO/GCE to interferent at physiological concentration.

To check the reproducibility of our manufacturing operation, we fabricate two electrodes in same condition and test their double layer capacitance (Cdl). Cyclic voltammograms were carried out in 0.1 M NaOH solution at scan rate from 10 to 100 mV s^{-1} (Figure 10a and b). Then the electrochemical active surface area was estimated by testing capacitive current at non-faraday region at different scan rates, from which double-layer charging (Cdl) was determined by plotting the $\Delta J = (J_a - J_c)$ at 0.10 V vs. Ag/AgCl against the scan rate as shown in Figure 10c and d. The linear slope is equivalent to twice of the Cdl, which can be used to represent the electrochemical active surface area [42]. From Figure 10c and d, it can be seen that the two fabricated electrodes have almost the same linear slope, revealing the same electrochemical active surface area of the two electrodes fabricated at same condition. That is, our fabrication process is reliable.

3.5. Practical applications

For practical analysis, the NiFe/GO/GCE was used to detect glucose concentration in human serum by amperometric measurement. Briefly, 20 μL serum was injected into 15 mL of 0.1 M NaOH solution, then the current response at +0.55 V on NiFe/GO/GCE was recorded. The recovery value was confirmed by standard injection of glucose with known concentration to the above sample, then record current at +0.55 V. As listed in Table 1, the recovery values of all three samples are close to 100%, indicating good practical application prospect of NiFe/GO/GCE electrode.

Table 1 Amperometric detection of glucose in serum

Sample	Concentration (mmol L^{-1})	RSD (%)	Added (mmol L^{-1})	Found (mmol L^{-1})	Recovery (%)
1	9.3	3.5	1	10.1	98
2	5.8	3.1	1	6.7	99
3	7.1	3.4	1	8.0	99

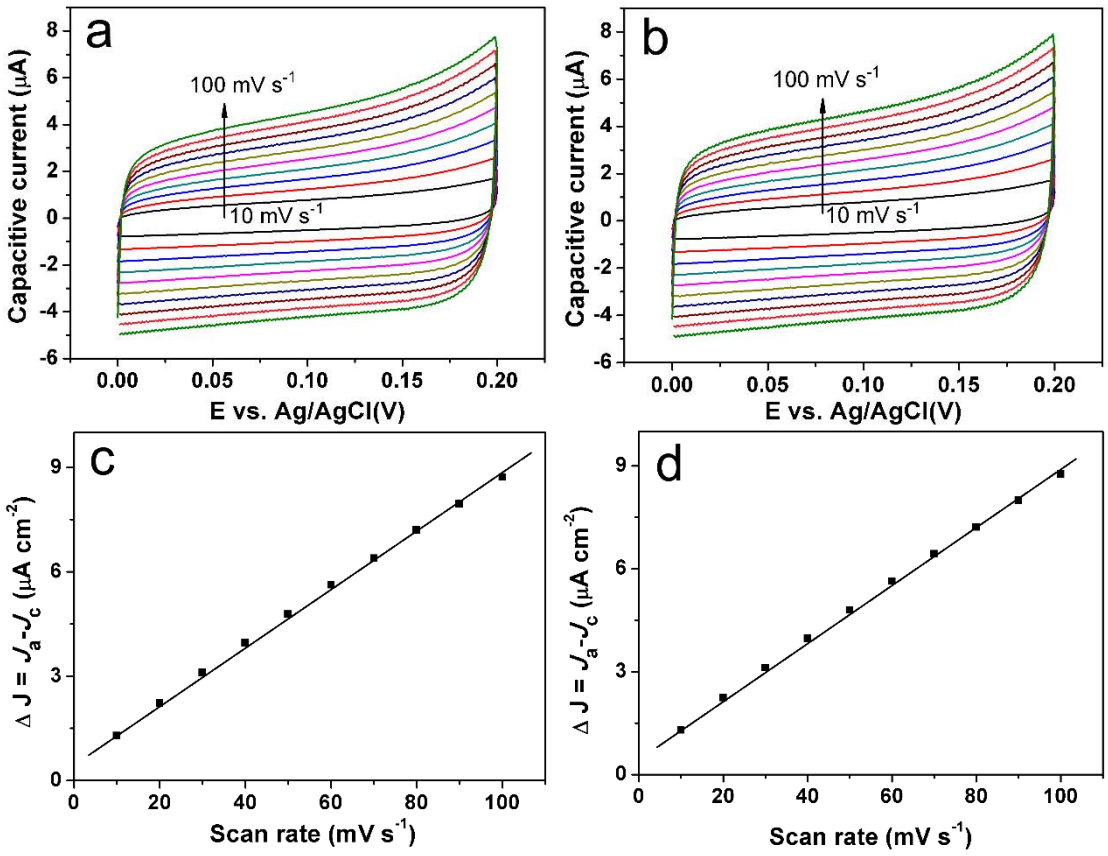

Figure 10. Cyclic voltammograms with different scan rates in potential range of 0.0 V to 0.2 V vs. Ag/AgCl where no Faradaic processes occur for first (A) and second fabrication (B) of electrode. Charging current density differences first (C) and second fabrication (D) of electrode plotted against scan rates.

4. Conclusions

In summary, a NiFe/GO/GCE electrochemical glucose sensor have successfully fabricated. The addition of Fe element into Ni nanoparticle to form NiFe alloy nanoparticle improved the electrochemical performance of glucose sensor. In addtion, the GO not only acts as support to load NiFe alloy from aggregation, but also play an important role for electronic transmission. The NiFe/GO/GCE electrode exhibited excellent sensitivity (173 μA $mM^{-1}cm^{-2}$) and wide detection linear range (up to 5 mM). In addition, NiFe/GO/GCE electrode shows high selectivity for glucose detection and can be applied to glucose detection in human serum. All results demonstrate that NiFe/GO/GCE electrode is a promising candidate in the development of cheap, stable and sensitive non-enzymatic glucose sensors.

Author Contributions: Data curation, Z.D.; Formal analysis, Z.D., Y.S. and J.D.; Investigation, Z.D., Y.S. and J.D.; Resources, Y.W.; Writing-Original Draft Preparation, Y.W. and Z.D.; Writing-review and editing, Z.D., Y.S. and Y.W.; Project Administration, Y.W.; Funding acquisition, J.D. All the authors discussed the results and commented on the manuscript.

Funding: This research was funded by the National Natural Science Foundation of China, grant number 21263023, Natural Science Foundation of Gansu Province, grant number 1606RJZA209, Central Universities Fundamental Research Foundation, grant number 31920160055, Youth Science Foundation of Gansu Province, grant number 17JR5RA282. The APC was funded by by the Natural Science Foundation of Gansu Province, grant number 17JR5RA172.

Acknowledgments: The authors will thank all the reviewers and editors for their great help and useful suggestions. Thank Jingwei Huang for his help for polishing the English writing.

Conflicts of Interest: The authors declare no conflict of interest.

References

1. Scognamiglio, V. Nanotechnology in glucose monitoring: advances and challenges in the last 10 years. *Biosens. Bioelectron.*, **2013**, *47C*, 12-25.
2. Clark, L.C.; Lyons, C. Electrode systems for continuous monitoring in cardiovascular surgery. *Ann. Ny. Acad. Sci.*, **1962**, *102*, 29-45.
3. Niu, X.H.; Shi, L.B.; Zhao, H.L.; Lan, M.B. Advanced strategies for improving the analytical performance of Pt-based nonenzymatic electrochemical glucose sensors: a minireview. *Anal. Methods*, **2016**, *8*, 1755-1764.
4. Gnana kumar, G.; Amala, G.; Gowtham, S.M. Recent advancements, key challenges and solutions in non-enzymatic electrochemical glucose sensors based on graphene platforms, *Rsc Adv.*, **2017**, *7*, 36949-36976.
5. Xie, J.D.; Gu, S.; Zhang, H. Microwave deposition of palladium catalysts on graphite spheres and reduced graphene oxide sheets for electrochemical glucose Sensing. *Sensors*, **2017**, *17*, 2163.
6. Yang, M.H.; Yang, Y.H.; Liu, Y.L.; Shen, G.L.; Yu, R.Q. Platinum nanoparticles-doped sol-gel/carbon nanotubes composite electrochemical sensors and biosensors. *Biosens. Bioelectron.*, **2006**, *21*, 1125-1131.
7. Niu, X.; Li, X.; Pan, J.; He, Y.; Qiu, F.; Yan, Y. Recent advances in non-enzymatic electrochemical glucose sensors based on non-precious transition metal materials: opportunities and challenges. *Rsc Adv.*, **2016**, *6*, 84893-84905.
8. Ma, L.; Wang, X.; Zhang, Q.; Tong, X.; Zhang, Y.; Li, Z. Pt catalyzed formation of a Ni@Pt/reduced graphene oxide nanocomposite: preparation and electrochemical sensing application for glucose detection. *Anal. Methods*, **2018**, *10*, 3845-3850.
9. Jin, L.; Meng, Z.; Zhang, Y.; Cai, S.; Zhang, Z.; Li, C.; Shang, L.; Shen, Y. Ultrasmall Pt nanoclusters as robust peroxidase mimics for colorimetric detection of glucose in human serum. *Acs Appl. Mater. Interfaces*, **2017**, *9*, 10027-10033.
10. Jiang, L.; Xue, Q.; Jiao, C.; Liu, H.; Zhou, Y.; Ma, H.; Yang, Q. A non-enzymatic nanoceria electrode for non-invasive glucose monitoring. *Anal. Methods*, **2018**, *10*, 2151-2159.
11. Zhao, W.; Zhang, R.; Xu, S.; Cai, J.; Zhu, X.; Zhu, Y.; Wei, W.; Liu, X.; Luo, J. Molecularly imprinted polymeric nanoparticles decorated with Au NPs for highly sensitive and selective glucose detection. *Biosens. Bioelectron.*, **2018**, *100*, 497-503.
12. Xiao, X.Y.; Montano, G.A.; Edwards, T.L.; Washburn, C.M.; Brozik, S.M.; Wheeler, D.R.; Burckel, D.B.; Polsky, R. Lithographically defined 3D nanoporous nonenzymatic glucose sensors. *Biosens. Bioelectron.*, **2011**, *26*, 3641-3646.
13. Wang, Q.; Wang, Q.; Qi, K.; Xue, T.; Liu, C.; Zheng, W.; Cui, X. In situ preparation of porous Pd nanotubes on a GCE for non-enzymatic electrochemical glucose sensors. *Anal. Methods*, **2015**, *7*, 8605-8610.
14. J. Wang, Electrochemical glucose biosensors. *Chem. Rev.*, **2008**, *108*, 814-825.
15. Huang, J.; He, Y.; Jin, J.; Li, Y.; Dong, Z.; Li, R. A novel glucose sensor based on MoS_2 nanosheet functionalized with Ni nanoparticles. *Electrochim. Acta*, **2014**, *136*, 41-46.
16. Shu, Y.; Yan, Y.; Chen, J.; Xu, Q.; Pang, H.; Hu, X. Ni and NiO nanoparticles decorated metal–organic framework nanosheets: facile synthesis and high-performance nonenzymatic glucose detection in human serum. *Acs Appl. Mater. Interfaces*, **2017**, *9*, 22342-22349.
17. Mao, Y.; Tian, S.; Gong, S.; Qin, Y.; Han, J.; Deng, S. A broad-spectrum sweet taste sensor based on $Ni(OH)_2$/Ni electrode. *Sensors*, **2018**, *18*, 2758.
18. Huang, M.; Luo, X.; He, D.; Jiang, P. Hierarchical $Co(OH)_2$ nanotube arrays grown on carbon cloth for use in non-enzymatic glucose sensing. *Anal. Methods*, **2017**, *9*, 5903-5909.
19. Huang, J.; Dong, Z.; Li, Y.; Li, J.; Wang, J.; Yang, H.; Li, S.; Guo, S.; Jin, J.; Li, R. High performance non-enzymatic glucose biosensor based on copper nanowires–carbon nanotubes hybrid for intracellular glucose study. *Sensor Actuat. B: chem.*, **2013**, *182*, 618-624.
20. Ma, J.; Wang, J.; Wang, M.; Zhang, G.; Peng, W.; Li, Y.; Fan, X.; Zhang, F. Preparation of cuprous oxide mesoporous spheres with different pore sizes for non-enzymatic glucose detection. *Nanomaterials*, **2018**, *8*, 73.

21. Huang, J.; Hu, G.; Ding, Y.; Pang, M.; Ma, B. Mn-doping and NiFe layered double hydroxide coating: Effective approaches to enhancing the performance of α-Fe_2O_3 in photoelectrochemical water oxidation. *J. Catal.*, **2016**, *340*, 261-269.
22. Yeh, T.H.; Liu, C.W.; Chen, H.S.; Wang, K.W. Preparation of carbon-supported PtM (M = Au, Pd, or Cu) nanorods and their application in oxygen reduction reaction. *Electrochem. Commun.*, **2013**, *31*, 125-128.
23. Sun, Y.; Yang, H.; Yu, X.; Meng, H.; Xu, X. A novel non-enzymatic amperometric glucose sensor based on a hollow Pt-Ni alloy nanotube array electrode with enhanced sensitivity. *Rsc Adv.*, **2015**, *5*, 70387-70394.
24. Chen, C.C.; Chen, L.C.; Synthesis and characterization of Pd-Ni core-shell nanocatalysts for alkaline glucose electrooxidation. *Rsc Adv.*, **2015**, *5*, 53333-53339.
25. Yang, J.; Liang, X.; Cui, L.; Liu, H.; Xie, J.; Liu, W. A novel non-enzymatic glucose sensor based on Pt_3Ru_1 alloy nanoparticles with high density of surface defects. *Biosens. Bioelectron.*, **2016**, *80*, 171-174.
26. He, W.; Sun, Y.; Xi, J.; Abdurhman, A.A.M.; Ren, J.; Duan, H. Printing graphene-carbon nanotube-ionic liquid gel on graphene paper: Towards flexible electrodes with efficient loading of PtAu alloy nanoparticles for electrochemical sensing of blood glucose. *Anal. Chim. Acta*, **2016**, *903*, 61-68.
27. Zhao, A.; Zhang, Z.; Zhang, P.; Xiao, S.; Wang, L.; Dong, Y.; Yuan, H.; Li, P.; Sun, Y.; Jiang, X.; Xiao, F. 3D nanoporous gold scaffold supported on graphene paper: Freestanding and flexible electrode with high loading of ultrafine PtCo alloy nanoparticles for electrochemical glucose sensing. *Anal. Chim. Acta*, **2016**, *938*, 63-71.
28. Suneesh, P.V.; Sara Vargis, V.; Ramachandran, T.; Nair, B.G.; Satheesh Babu, T.G. Co–Cu alloy nanoparticles decorated TiO_2 nanotube arrays for highly sensitive and selective nonenzymatic sensing of glucose. *Sensor Actuat. B: chem.*, **2015**, *215*, 337-344.
29. Sheng, Q.; Liu, D.; Zheng, J. NiCo alloy nanoparticles anchored on polypyrrole/reduced graphene oxide nanocomposites for nonenzymatic glucose sensing. *New J. Chem.*, **2016**, *40*, 6658-6665.
30. Han, B.; Pan, M.; Zhou, J.; Wang, Y.; Wang, Z.; Jiao, J.; Zhang, C.; Chen, Q. Facile synthesis of β-Lactoglobulin-Functionalized reduced graphene oxide and trimetallic PtAuPd nanocomposite for electrochemical sensing. *Nanomaterials*, **2018**, *8*, 724.
31. Jiang, L.C.; Zhang, W.D. A highly sensitive nonenzymatic glucose sensor based on CuO nanoparticles-modified carbon nanotube electrode. *Biosens. Bioelectron.*, **2010**, *25*, 1402-1407.
32. Wu, H.X.; Cao, W.M.; Li, Y.; Liu, G.; Wen, Y.; Yang, H.F.; Yang, S.P. In situ growth of copper nanoparticles on multiwalled carbon nanotubes and their application as non-enzymatic glucose sensor materials. *Electrochim. Acta*, **2010**, *55*, 3734-3740.
33. Novoselov, K.S.; Geim, A.K.; Morozov, S.V.; Jiang, D.; Zhang, Y.; Dubonos, S.V.; Grigorieva, I.V.; Firsov, A.A. Electric field effect in atomically thin carbon films. *Science*, **2004**, *306*, 666-669.
34. Radhakrishnan, S.; Kim, S.J. Facile fabrication of NiS and a reduced graphene oxide hybrid film for nonenzymatic detection of glucose. *Rsc Adv.*, **2015**, *5*, 44346-44352.
35. Yan, X.; Gu, Y.; Li, C.; Zheng, B.; Li, Y.; Zhang, T.; Zhang, Z.; Yang, M. A non-enzymatic glucose sensor based on the CuS nanoflakes–reduced graphene oxide nanocomposite, *Anal. Methods*, **2018**, *10*, 381-388.
36. Yu, X.; Yang, P.; Chen, S.; Zhang, M.; Shi, G. NiFe alloy protected silicon photoanode for efficient water splitting. *Adv. Energy Mater.*, **2017**, *7*, 1601805.
37. Bin, D.; Yang, B.; Li, C.; Liu, Y.; Zhang, X.; Wang, Y.; Xia, Y. In situ growth of NiFe alloy nanoparticles embedded into N-doped bamboo-like carbon nanotubes as a bifunctional electrocatalyst for Zn-Air batteries. *Acs Appl. Mater. Interfaces*, **2018**, *10*, 26178-26187.
38. Wang, G.; Zheng, D.; Liu, D.; Harris, J.; Si, J.; Ding, T.; Qu, D. Highly efficient Ni-Fe based oxygen evolution catalyst prepared by a novel pulse electrochemical approach. *Electrochim. Acta*, **2017**, *247*, 722-729.
39. Torabinejad, V.; Aliofkhazraei, M.; Assareh, S.; Allahyarzadeh, M.H.; Rouhaghdam, A.S. Electrodeposition of Ni-Fe alloys, composites, and nano coatings-a review. *J. Alloy. Compd.*, **2017**, *691*, 841-859.
40. Hummers Jr, W.S.; Offeman, R.E. Preparation of graphitic oxide. *J. Am. Chem. Soc.*, **1958**, *80*, 1339-1339.
41. Li, J.; Tang, W.; Huang, J.; Jin, J.; Ma, J. Polyethyleneimine decorated graphene oxide-supported $Ni_{1-x}Fe_x$ bimetallic nanoparticles as efficient and robust electrocatalysts for hydrazine fuel cells. *Catal. Sci. Technol.*, **2013**, *3*, 3155-3162.
42. Song, F.; Hu, X. Ultrathin cobalt-manganese layered souble hydroxide is an efficient oxygen evolution catalyst. *J. Am. Chem. Soc.*, **2014**, *136*, 16481-16484.